

## Article

# The Lipidome of the Gastrointestinal Tract in Lactating Holstein Cows

Qianming Jiang <sup>1</sup>  and Juan J. Loor <sup>1,2,\*</sup> <sup>1</sup> Department of Animal Sciences, University of Illinois, Urbana, IL 61801, USA<sup>2</sup> Division of Nutritional Sciences, University of Illinois, Urbana, IL 61801, USA

\* Correspondence: jloor@illinois.edu

**Abstract:** The lipidome is a key determinant of structural and functional characteristics of tissues, contributing to optimal gut function and efficiency of nutrient use in the gastrointestinal tract (GIT). Our objective was to study lipidomic profiles in different sections of the GIT in lactating dairy cows and to link them with biological functions. We studied the lipid species in ruminal papillae and epithelium from duodenum, jejunum, and ileum harvested after slaughter from five lactating Holstein cows. Extracted lipids were identified by LC/MS/MS and analyzed via Lipidsearch, Metaboanalyst 5.0, and lipid ontology (LION). Of 1259 lipid species identified across the GIT, 387, 565, 193, and 86 were neutral lipids, phospholipids, sphingolipids, and derivatized lipids, respectively. Among the 1223 lipid species common to the GIT, a PLS-DA analysis revealed similar profiles for jejunum and ileum and discriminated them from rumen and duodenum. The content of 12 out of 28 lipid classes differed ( $p < 0.05$ ) among GIT sections. The average fatty acid chain length in lipid species spanned from 9 to 37 carbons, and the average degree of unsaturation ranged from 0 to 6. The term ‘membrane component’ from LION analysis differed markedly between the rumen and the small intestine. Future studies will help better understand what factors (function or cellular component) in a given section of the GIT are related to the different lipid species. This is the first description of the lipidome profiles across sections of the GIT in lactating dairy cows. The unique lipidome profiles uncovered distinct structural and functional properties across the bovine GIT, which may impact the efficiency of nutrient use.



**Citation:** Jiang, Q.; Loor, J.J. The Lipidome of the Gastrointestinal Tract in Lactating Holstein Cows. *Ruminants* **2023**, *3*, 76–91. <https://doi.org/10.3390/ruminants3010007>

Academic Editors: Ana Isabel Roca-Fernández and Magdalena Arévalo-Turrubiarte

Received: 26 January 2023  
Revised: 16 March 2023  
Accepted: 16 March 2023  
Published: 20 March 2023



**Copyright:** © 2023 by the authors. Licensee MDPI, Basel, Switzerland. This article is an open access article distributed under the terms and conditions of the Creative Commons Attribution (CC BY) license (<https://creativecommons.org/licenses/by/4.0/>).

**Keywords:** lipid profiles; nutrition; rumen; small intestine; bovine

## 1. Introduction

Lipids play a crucial role in an animal’s body and are the essential components of the membrane systems, including the cell membrane [1], endoplasmic reticulum (ER) [2], Golgi apparatus (GA), mitochondrial membrane, and vesicles [3]. The double layer of the cell membrane separates the cell contents from the extracellular matrix and plays a role in molecular transport. The different lipid species associated with the ER, GA, and mitochondria support the biological processes of living cells [4]. Phospholipids, the major components of the cell membrane system, form the lipid bilayer in the cell membrane system [5].

Within the enterocytes, a phospholipid monolayer decorated by proteins encapsulates the neutral lipids forming the lipid droplet (LD) in intestinal enterocytes [6] and adipose tissue [7]. The neutral lipids mainly include cholesteryl ester (ChE), triacylglycerol (TG), diglyceride (DG), and monoglyceride (MG). The absorbed dietary lipids from the intestinal lumen are used to synthesize chylomicrons and transport them into the lymph system and then the blood [6]. The fatty acids (FA) released from plasma lipoproteins are transported into cells for esterification into TG or for beta-oxidation to provide energy [8,9].

Various lipids can act as signaling molecules that regulate the metabolism of cells [4]. For instance, sphingolipids have important roles in membrane and lipoprotein structure

and act as second messengers for differentiation factors, cytokines, growth factors, and a growing list of agonists [10]. Sphingolipids play a role in cellular processes such as cell movement, membrane homeostasis, nutrient transport, endocytosis, and protein synthesis. Ceramide (Cer), sphingosine, and sphingosine-1-phosphate, subclasses of sphingolipids, regulate Gq/IP3/Ca<sup>2+</sup> and G12/13/Rho/ROCK signaling pathways [11]. Acylcarnitines (AcCa) transport long-chain fatty acids (LCFA), and plasmalogens exert antioxidant functions [12]. Clearly, to better appreciate the potential role of the various lipid species found in the GIT in the context of function requires a high-throughput approach. Lipidomics is a powerful technology for studying all lipid species with mass spectrometry (MS).

The present study aimed to generate the first lipidome profiles of different sections of the bovine GIT and to link them with biological functions. The use of lactating and high-producing Holstein dairy cows provided an ideal opportunity to generate fundamental knowledge of the unique lipidome features of the rumen and the small intestine. These sections of the GIT have unique functions in the context of nutrient digestion and absorption. The lipidome approach would allow an initial exploration of the potential functions conferred by the lipid species detected in sections of the GIT. Our general hypothesis was that different sections of GIT have unique lipid profiles that confer unique functions.

## 2. Materials and Methods

### 2.1. Animal Handling and Experimental Design

The Institutional Animal Care and Use Committee (IACUC) at the University of Illinois approved the slaughter of the cows via captive bolt (#19161). Five healthy non-pregnant mid-lactation multiparous Holstein cows ( $3.40 \pm 0.74$  parities;  $2.99 \pm 0.09$  body condition score;  $759 \pm 17$  kg body weight) that were housed comingled with other cows in the University of Illinois Dairy Unit herd in free stalls with sand bedding and milked twice per day were selected. These cows were free of clinical disease, were culled due to failure to become pregnant, and were fed a typical total mixed ration composed of corn silage/alfalfa hay with water provided ad libitum. They averaged  $136 \pm 3$  days in milk and  $37 \pm 6$  kg milk/d before slaughter. The diet fed contained 17.4% crude protein, 1.74 Mcal/kg net energy for lactation, and 358 g/d methionine in the metabolizable protein (Supplementary Materials File Table S1) and was delivered to the feed bunk at 06:00 and 17:30 h daily. The day of sacrifice (06:00 h), cows were given 300 mg Xylazine intramuscularly to sedate (Rompun<sup>®</sup>, 100 mg/mL, Dechra, Kansas City, KS, USA), loaded two at a time into a livestock trailer (EBY Maverick LS livestock trailer, EBY, Seymour, IN, USA), and transported 0.8 km from the University of Illinois Dairy Unit to the Veterinary Diagnostics Laboratory, University of Illinois College of Veterinary Medicine, Urbana-Champaign. Cows became recumbent within 10 min of injection and were then euthanized with a penetrating captive bolt and removed from the trailer. Cows were then exsanguinated and within 10 min the body cavity was opened to gain access to the gut tissues.

### 2.2. Sample Collection

Tissue samples were harvested within 20 min from sacrifice. The ruminal papillae from the ventral sac of the rumen were harvested using surgical scissors. The small intestine was cut from the rumen and placed on a necropsy table where duodenal tissue was collected approximately 25 cm distal from the pyloric sphincter; jejunum was collected approximately 1 m proximal to the ileocecal junction, and the ileum approximately 18 cm proximal to the ileocecal junction [13]. Twenty-five cm segments from the duodenum, jejunum, and ileum were cut into pieces measuring approximately 10 cm × 20 cm and washed with phosphate-buffered saline to avoid food and microbial contamination. Then, a sterile scalpel blade was used to scrape the epithelium. Samples were collected into cryo-vials and immediately frozen in liquid nitrogen. Afterward, the tissues were transported to the laboratory and stored at  $-80$  °C.

### 2.3. Lipid Extraction and Lipidomics

Lipids were extracted according to a previous protocol [14]. Briefly, approximately 30 mg of tissue was homogenized with 150  $\mu$ L cold LC-MS grade methanol and 450  $\mu$ L Methyl-tert-butyl-ether (MTBE). Three-hundred  $\mu$ L 25% cold LC-MS grade methanol was added to the samples and vortexed. After centrifugation at  $14,000\times g$  for 10 min, the supernatant was transferred to a fresh 10 mL glass tube and dried under a nitrogen gas stream. Lastly, the dried samples were redissolved in 250  $\mu$ L acetonitrile/isopropanol (*v/v*, 7:3). Samples were then delivered to the Roy J. Carver Biotechnology Center, University of Illinois (Urbana) and used for Lipid profiling analysis by LC/MS/MS and Lipidsearch (Thermo-Fisher Sci, Waltham, MA, USA) [15].

### 2.4. Functional Mapping

After removing lipid species that could not be mapped against the lipid ontology (LION) [16], signal counts for individual molecular species were input for data formatting (replace 0 and/or NAs and the sample normalized by the sum of each sample) and enrichment in Ranking mode. A total of 1065 out of 1070 (99.53%) identifiers were matched to LION. The LION term and coordinate lipid species were mapped and reported in Supplementary File Table S2.

### 2.5. Statistical Analysis

The raw data were normalized by signal counts (to internal standard signals and sample weight). Lipid classifications and distribution bar plots were drawn with Sigma Plot (version 14.0; Systat Software Inc., San Jose, CA, USA). The total lipid content for each section of the GIT was calculated as the sum of signal counts for individual molecular species [15]. The average chain length and average unsaturation of FA were calculated taking into account all the carbons, and the degree of total unsaturation for each lipid species was divided by the chain number for each species and rounded to an integer number. Then, the signal counts of lipid species were summed for each term of average chain length, average unsaturation, and LION. The sum of signal counts for each term was then log<sub>2</sub> transformed. The resulting data were analyzed using PROC MIXED in SAS OnDemand for Academics (SAS Institute Inc., Cary, NC, USA) <https://welcome.oda.sas.com/login> (accessed on 13 February 2022). The model tested the fixed effect of GIT section and statistical differences were determined using pairwise comparisons. SAS results were read in Matlab to extract the least squares means, standard errors of the means, and *p*-value. Heatmaps were drawn in R pheatmap with the (1.0.12) package. Log<sub>2</sub> transformed lipid species data in all sections of the GIT were analyzed using Metaboanalyst 5.0 (<https://www.metaboanalyst.ca/docs/Format.xhtml>) [17]. By default, missing values were replaced with 1/5 of the minimum positive values of their corresponding variables, and Partial Least Squares Discriminant Analysis (PLS-DA) for the 2D scores plot was performed.

## 3. Results and Discussion

### 3.1. Overall Lipid Classification and Distribution

The untargeted lipidomic analyses detected 1259 lipid species in total, with 387 neutral lipids, 565 phospholipids, 193 sphingolipids, 86 derivatized lipids (biotinylation, diazomethane), and 28 fatty acyl and other lipids (Figure 1A). Among all the lipid species, the most abundant group was phospholipid, with 12 classes. Next were neutral lipids and sphingolipids, with five and four classes (Supplementary File Table S3).

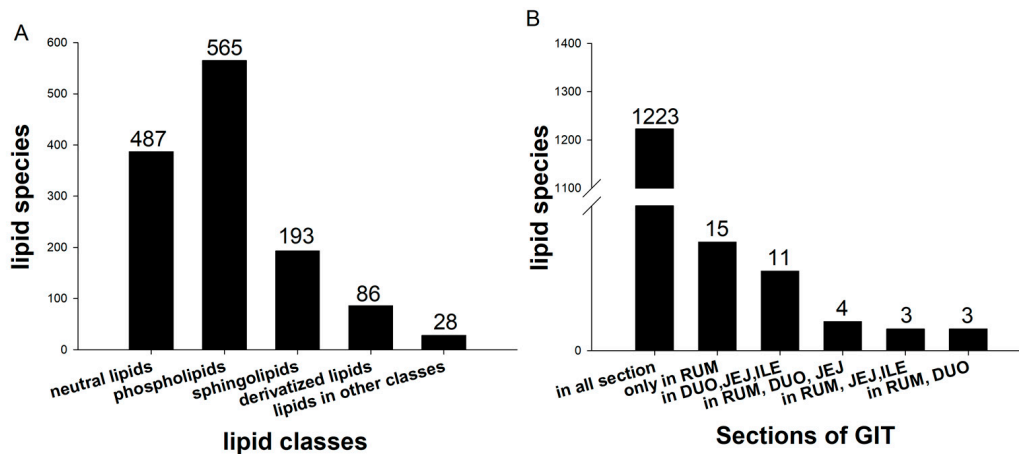


**Figure 1.** Classification (A) and distribution (B) of a total of 1259 lipid species identified across the ruminal papillae and epithelium from duodenum, jejunum, and ileum of 5 lactating Holstein cows.

There were 1223 lipids in the rumen, duodenum, jejunum, and ileum. Fifteen lipids only exist in the rumen, which includes one neutral lipid, six phospholipids, two sphingolipids, and six derivatized lipids. Eleven lipid species only existed in the small intestine; four lipid species existed in rumen, duodenum, and jejunum, but not ileum; three lipid species existed in rumen, jejunum, ileum, but not duodenum; three lipid species only existed in rumen and duodenum (Figure 1B, Supplementary Materials Tables S4 and S5).

In the PLS-DA, the rumen and duodenum were separated from the ileum and jejunum (Figure 2). Lipid species with top variable importance in projection (VIP) scores were phosphatidylglycerol (34:2), triglyceride (20:4\_20:4\_20:4), phosphatidylglycerol (20:5\_20:4), acyl carnitine (22:2), and phosphatidylcholine (38:0 e) (Supplementary File Table S6). The general analysis showed that lipid species’ composition was more similar in jejunum and ileum, while the rumen and duodenum tended to have unique profiles.

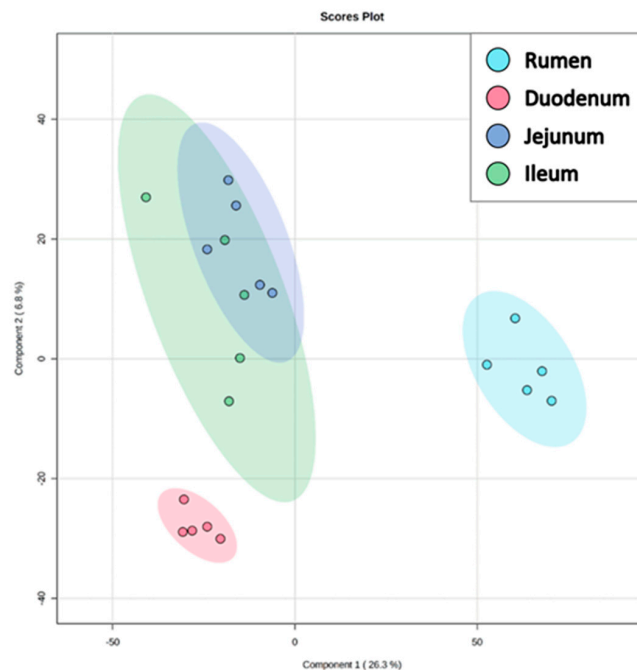


**Figure 2.** Partial Least Squares Discriminant Analysis (PLS-DA) of common lipid species identified across the ruminal papillae and epithelium from duodenum, jejunum, and ileum of 5 lactating Holstein cows.

In a previous study, lipidomic data from blood revealed differences in phosphatidylglycerol (PG), phosphatidylcholine (PC), sphingomyelin (SM), and TG between cow plasma and calf serum. Compared with colostrum, the cow plasma or calf serum had a greater percentage of PC, phosphatidylinositol (PI), and SM, but a lower percentage of PG [18]. Dynamic changes in plasma lipidomic were also observed in the transition to lactation, where both C 36:6 and PC 32:3 were identified as potential biomarkers for the increase in lipolysis, ketogenesis, and hepatic lipid deposition after parturition [19].

Although few lipid composition data of the rumen and intestine in dairy cows are published, the lipid composition of the intestine was reported for rats, pigs, and rabbits. The rat Golgi membrane of the small intestine contains 26.9% PC, 16.1% cholesterol, 13.2% phosphatidylethanolamine (PE), 12.0% FA, and 10.4% SM (*w/w*) of total lipids. Other lipids include ChE, TG, PI, phosphatidylserine (PS), lysophosphatidylcholine (LPC), and cardiolipin (CL); the detected carbon numbers of FA ranged from 14–20 [20]. In the jejunal brush border membrane of the rat, the main types of lipids were phospholipids, neutral glycolipids, cholesterol, TG, FA, gangliosides, MG, bile acids, and the phospholipids LPC, SM, PC, PS, PI, PE, CL, and lecithin [21,22]. The lipid composition of small intestinal brush border membrane can be altered by age [21], glucocorticoids [23], fasting, and diabetes [22]. Rat jejunal and ileal microvillus membrane phospholipid contained ~23–31% PE, ~18–31% PC, ~16–30% PS, ~10–22% SM, ~3–4%LPC, and ~2–7% PI % of total lipid phosphorous [24]. Compared with another similar study that only measured PE, PC, PS, SM, and LPC of isolated microvilli membranes [25], the content of total phospholipids was slightly different. The 14-, 16-, 18-, and 20-carbon FA were detected in rat jejunal and ileal microvilli membranes [24]. Cholesterol, ChE, phospholipids, TG, cerebrosides, and gangliosides were detected in the intestinal mucus of rats, and their fractions could be altered by chronic ethanol feeding [26].

In the basolateral plasma membrane of pig intestinal mucosal cells, the main lipid classes were phospholipids and cholesterol, and the phospholipids include ~45% PC, ~31% PE, ~9% PS, ~7% SM, and ~6% PI *w/w* of total phospholipid phosphorous; the major carbon numbers of detected FA in PC and PE were 14–24 [27]. The pig intestinal brush border membrane contains ~33–40% PC, ~37–41% PE, ~8–12% PS, ~7–8% SM, ~4–5% PI, ~1–2% LPC, and ~1% of total phospholipids as diphosphatidylglycerol. The FA with 14-, 16-, 18-, 20-, 22-, 24-carbons were detected in these phospholipids [28]. In the jejunal and ileal mucosa of piglets, phospholipids contain ~46–51 mol PC, ~32–41 mol PE, ~9–11 mol SM, ~0.9–2 mol PS, ~0.3–4 mol LPC, and ~0.2–4 mol PI of 100 mol total phospholipids, and they were altered by malnutrition [29].

The rabbit jejunal and ileal basolateral membrane contains cholesterol and phospholipids containing ~33–60% PE, ~13–22% PC, ~12–15% PS, ~12–23% PI, and ~8–17% SM [30]. The rabbit small intestinal brush border membrane contained ~0.5 mg total lipid/mg protein, ~50 µg cholesterol/mg protein, and ~8 µg lipid phosphorous/mg protein; the phospholipids contained phosphatidic acid (PA), PE, ethanolamine plasmalogen, alkylacylglycerophosphoethanolamine, PS, lysophosphatidylethanolamine (LPE), PC, alkyl and alkenylglycerophosphocholine, LPC, PI, and SM; the neutral lipids contained cholesterol, ChE, DG, TG, and FA [31].

In previous studies, specific parts of the membrane were isolated from intestinal cells, and the different lipid compositions were studied. The cell membrane mainly consists of cholesterol and phospholipids [21,31], and the main phospholipid classes were PE, PC, PS, PI, and SM. Clearly, the use of more robust techniques such as LC/MS/MS to analyze the lipidome in the present study allowed us to detect more lipid species and their profiles in the major sections of the GIT. One limitation of the present study is that we could not separate the brush border membrane from the basolateral membrane of intestinal cells. Thus, future research could help ascertain if these membranes have unique lipid profiles and how those confer unique physiological functions to the tissue.

### 3.2. Lipid Content Profiles

The lipid content across the GIT is reported in Table 1. Across 28 lipid classes, the lipid content of 12 lipid classes was significantly different among the 4 sections of GIT, with lipid content of 14 lipid classes in the rumen being significantly different compared with the small intestine. The content of CL, monolysocardiolipin (MLCL), LPC, dimethyl phosphatidylethanolamine, lysodimethylphosphatidylethanolamine, AcCa, and cyclic PA in the rumen was lower than in the small intestine ( $p < 0.05$ ). In contrast, the lipid content of PE, DG, cholesterol ester, Cer, ceramide phosphate, ceramide phosphoethanolamines, methyl phosphatidylcholine (MePC), and coenzyme in the rumen was greater than in the small intestine ( $p < 0.05$ ). ChE content was lower in duodenum and jejunum ( $p < 0.05$ ). The zymosterol ester (ZyE) was the greatest in the duodenum ( $p < 0.05$ ). Dimethyl phosphatidylethanolamine content was greater in the duodenum and jejunum ( $p < 0.05$ ). Cardiolipins (CL), localized and synthesized in the inner mitochondrial membrane [32], contains four fatty acyl chains and a lipid dimer consisting of two phosphatidyl residues bridged by glycerol [33,34]. Most of the published studies of CL are related to the high density of proteins in the inner mitochondrial membrane. The mitochondria lacking CL failed to generate ATP during stressful conditions and destabilized the respiratory super complexes [35]. The CL stabilizes the tertiary structure of proteins, such as the ADP/ATP carrier, helps support the proton conduction of protein complexes, and increases super complex association and the arrangement of the protein complex [34]. Monolysocardiolipin (MLCL) is generated during the degradation of CL through the action of phospholipases [34]. The fact that MLCL and CL content was greater in the small intestine than in the rumen ( $p < 0.05$ ) suggested that mitochondria in the small intestine have a greater amount of inner membrane, likely because absorptive and metabolic processes in this section of the GIT require higher levels of energy consumption [36]. The PE content was greater in the rumen than the intestine, the LPC content was greater in the small intestine than the rumen ( $p < 0.05$ ), and the PC content tended to be greater in the small intestine ( $p = 0.06$ ). The PC content was markedly greater, ranging from 52–60%, followed by TG at 15–21% (Table 1). Of the published data available in bovine, similar analysis to ours revealed that in milk, the relative proportion of TG was ~4-to-10-fold greater than other lipid classes, including PC, DG, and Cer [37,38]. Furthermore, the milk lipidomic profiling was altered by subclinical intramammary infection and dietary supplementation of citrus peel extract and *Eucommia ulmoides* leaves [37–39]. Additional research might be warranted to explore how disease and nutrition could alter the GIT lipidome and the functional outcomes.

The primary structural lipid class in eukaryotic membranes are the glycerophospholipids, including PC (over 50% of phospholipids), PE (around 20% of phospholipids), PS, PI, and PA. The distributions of phospholipids are different in the plasma membrane, ER, mitochondria, GA, and endosomes [4]. The ER is the main site of lipid synthesis, including phospholipids, cholesterol, and Cer; the GA synthesizes sphingolipid and produces SM, glucosylceramide (GlcCer), lactosylceramide (LacCer), and higher-order GSLs, and these lipids are primarily transported to the plasma membrane [4]. LPC, LPE, Lysophosphatidylglycerol (LPG), and Lysophosphatidylinositol (LPI) result from the hydrolysis of PC, PE, PG, and PI. These molecules can serve as signal mediators by attaching to specific receptors and changing various cellular functions and metabolism [40–42]. The PC and PE are hydrolyzed to lysophospholipids and glycerophosphoryl bases before absorption in the rat [43]. Thus, the differences we detected for PE, LPC, and PC, for example, among sections of the GIT, indicated that unique epithelial membrane composition likely is associated with a unique function.

**Table 1.** Relative abundance, SEM, and *p*-value of common lipid classes across the ruminal papillae and epithelium from duodenum, jejunum, and ileum of 5 lactating Holstein cows.

Class Group	Class Name	Rumen%	Duodenum%	Jejunum%	Ileum%	SEM	<i>p</i> -Value	DIJ * vs. Rumen
Phospholipids	Cardiolipin	0.118	0.154	0.151	0.152	0.000150	0.20	0.04
	Monolysocardiolipin	0.022 <sup>b</sup>	0.089 <sup>a</sup>	0.072 <sup>a</sup>	0.078 <sup>a</sup>	0.000194	0.01	<0.01
	Phosphatidylcholine	52.4	54.0	60.2	58.2	0.024640	0.07	0.06
	Phosphatidylethanolamine	6.009	4.180	5.112	5.170	0.004848	0.08	0.04
	Phosphatidylethanol	0.003	0.002	0.002	0.003	0.000004	0.18	0.32
	Phosphatidylserine	1.591	1.502	1.388	1.410	0.001011	0.49	0.20
	Phosphatidylglycerol	0.102	0.088	0.104	0.112	0.000150	0.42	0.95
	Phosphatidylinositol	0.059	0.067	0.067	0.077	0.000129	0.77	0.42
	Lysophosphatidylcholine	0.562 <sup>b</sup>	1.953 <sup>a</sup>	1.578 <sup>a</sup>	1.703 <sup>a</sup>	0.004832	0.05	0.01
	Lysophosphatidylethanolamine	0.060	0.041	0.045	0.058	0.000159	0.55	0.34
	Lysophosphatidylglycerol	0.001	0.001	0.001	0.001	0.000003	0.37	0.11
	Lysophosphatidylinositol	<0.001	<0.001	0.001	<0.001	0.000002	0.41	0.43
Neutral lipids	Monoglyceride	0.074	0.065	0.058	0.093	0.000100	0.10	0.85
	Diglyceride	1.026 <sup>a</sup>	0.684 <sup>b</sup>	0.645 <sup>b</sup>	0.707 <sup>b</sup>	0.000684	<0.01	<0.01
	Triglyceride	20.6	20.6	15.9	16.4	0.031940	0.59	0.43
	Cholesterol Ester	0.072 <sup>a</sup>	0.012 <sup>c</sup>	0.023 <sup>bc</sup>	0.028 <sup>b</sup>	0.000050	<0.01	<0.01
	Zymosterol Ester	0.016 <sup>b</sup>	0.091 <sup>a</sup>	0.021 <sup>b</sup>	0.012 <sup>b</sup>	0.000115	<0.01	0.07
Sphingolipids	Ceramides	1.037 <sup>a</sup>	0.612 <sup>b</sup>	0.500 <sup>b</sup>	0.533 <sup>b</sup>	0.000581	<0.01	<0.01
	Ceramides phosphate	0.003 <sup>a</sup>	<0.001 <sup>b</sup>	<0.001 <sup>b</sup>	<0.001 <sup>b</sup>	0.000003	<0.01	<0.01
	Ceramide phosphoethanolamines	0.001	<0.001	0.001	0.001	0.000002	0.17	0.03
	Sphingomyelin	9.348	9.501	8.615	10.210	0.013140	0.86	0.95
Derivatized lipids (biotinylation, diazomethane)	Bis-methyl phosphatidic acid	2.457	2.169	1.924	1.614	0.002693	0.16	0.08
	Dimethyl phosphatidylethanolamine	0.086 <sup>b</sup>	0.147 <sup>a</sup>	0.150 <sup>a</sup>	0.113 <sup>b</sup>	0.000113	<0.01	<0.01
	Lysodimethylphosphatidylethanolamine	0.003 <sup>b</sup>	0.013 <sup>a</sup>	0.010 <sup>a</sup>	0.010 <sup>a</sup>	0.000028	0.02	<0.01
	Methyl phosphatidylcholine	3.807 <sup>a</sup>	3.580 <sup>ab</sup>	3.104 <sup>bc</sup>	2.886 <sup>c</sup>	0.001793	0.01	0.01
Fatty acyl and other lipids	Acyl Carnitine	0.032 <sup>c</sup>	0.094 <sup>a</sup>	0.052 <sup>bc</sup>	0.082 <sup>ab</sup>	0.000143	0.02	0.01
	Coenzyme	0.492 <sup>a</sup>	0.344 <sup>b</sup>	0.282 <sup>b</sup>	0.349 <sup>b</sup>	0.000338	<0.01	<0.01
	Cyclic phosphatidic acid	0.0001	0.0011	0.0016	0.0014	0.000005	0.07	0.01

\* DIJ = combination of duodenum, jejunum, and ileum, <sup>a,b,c</sup> Means on the same row differ (*p* < 0.05).

The dietary ChE is hydrolyzed to cholesterol and FA by cholesterol esterase [44]. The absorbed cholesterol is esterified by acetyl-CoA cholesterol-acetyltransferase within the intestinal cells [45]. Cholesterol is also a component of cell membranes, and its level may change the permeability of cellular membranes [46]. There are no data demonstrating that cholesterol or ChE can be absorbed from the rumen during digestion. Traditionally, the rumen is only considered to play a role in the absorption of volatile fatty acids [47]. Thus, it is unclear if the greater overall ChE content in the rumen, compared to the small intestine, is associated with a specific function.

Previous studies revealed that high-grain diets alter the abundance of genes associated with cholesterol homeostasis in ruminal papillae of dairy cows [46], suggesting that increased cellular cholesterol may be a sign of inflammation and increased cell proliferation [46,48,49]. In plants, vitamin D is synthesized from cholesterol and zymosterol [50]. Zymosterol is also an intermediate of ergosterol, cholesterol, campesterol, and stigmasterol in fungi and bacteria [51]. Thus, we infer that feed and microbial cells contribute zymosterol to the digesta available for digestion and absorption. Although the content of cholesterol increases and ZyE decreases gradually from duodenum to jejunum to ileum, it is unknown at which section of the GIT zymosterol is digested or absorbed. Based on available knowledge, it can be inferred that ZyE, along with cholesterol, FA, and MG, are absorbed in the jejunum. The fact that ZyE concentrations were lower in the jejunum may suggest this molecule is metabolized rapidly within the enterocytes or transported into the circulation. The greater DG in the rumen, compared to the small intestine, coupled with the lack of difference in MG and TG content across sections of the GIT suggested that DG may have specific functions in the rumen.

Ceramide (Cer) de novo synthesis occurs in the ER of the gut and uses sphingoid bases, palmitoyl-CoA, and serine. The complex sphingolipids, including SM, glucosylceramides, and gangliosides, are produced by the GA from Cer [52]. In humans and rats, Cer and/or its metabolites regulate proliferation, differentiation, and apoptosis in epidermal keratinocytes and contribute to innate immune function [53,54]. Cer also plays a crucial role in numerous physiologic and pathologic processes in the gut [52], and the accumulation of Cer in the intestine led to inflammation and cell death in mice [55]. The different Cer and Cer concentrations between the rumen and intestine could be associated with different cellular processes in each section.

Carnitine is a molecule that helps transport LCFA from the cytosol to the mitochondria for oxidation. The small intestine had a greater content of AcCa compared to the rumen, indicating a higher reliance in these sections of the GIT on LCFA transport and metabolism [56]. Although this is a novel outcome of the present study, it is important to recognize that the intestinal epithelial cells have other energy sources, such as glutamate, glutamine, glucose [57], and butyrate [58].

### 3.3. Chain Length and Unsaturation of Fatty Acids

The average chain length of FA in each lipid class is depicted in Figure 3; details are in the Supplementary File Table S7. Among phospholipids, PC had the highest signal counts among species with mainly 15 to 21 carbons in chain length (Figure 3A). Next was PE, with an average of mainly 17 to 19 carbons, and PS, with an average of mainly 18 to 20 carbons. The chain length of FA ranged from 9 to 22 carbons for the phospholipids. Among neutral lipids, the majority of TG signal counts ranged from FA with 15 to 20 carbons (Figure 3B). The FA chain length of neutral lipids ranged from 9 to 37 carbons. The ChE and ZyE had longer FA with up to an average of 30 and 37 carbons. The SM had the highest signal counts, averaging 17 to 22 carbons (Figure 3C). Next was the Cer with 17 to 22 carbons. Bis-methyl phosphatidic acid (BisMePA) signal counts were highest with 18 to 20 carbons, and MePC signal counts were highest with 16 to 18 carbons. The average FA chain length for all the lipids we measured was mainly from 13 to 23 carbons, and ChE and ZyE included very long chain fatty acids ( $\geq 22$  carbon).

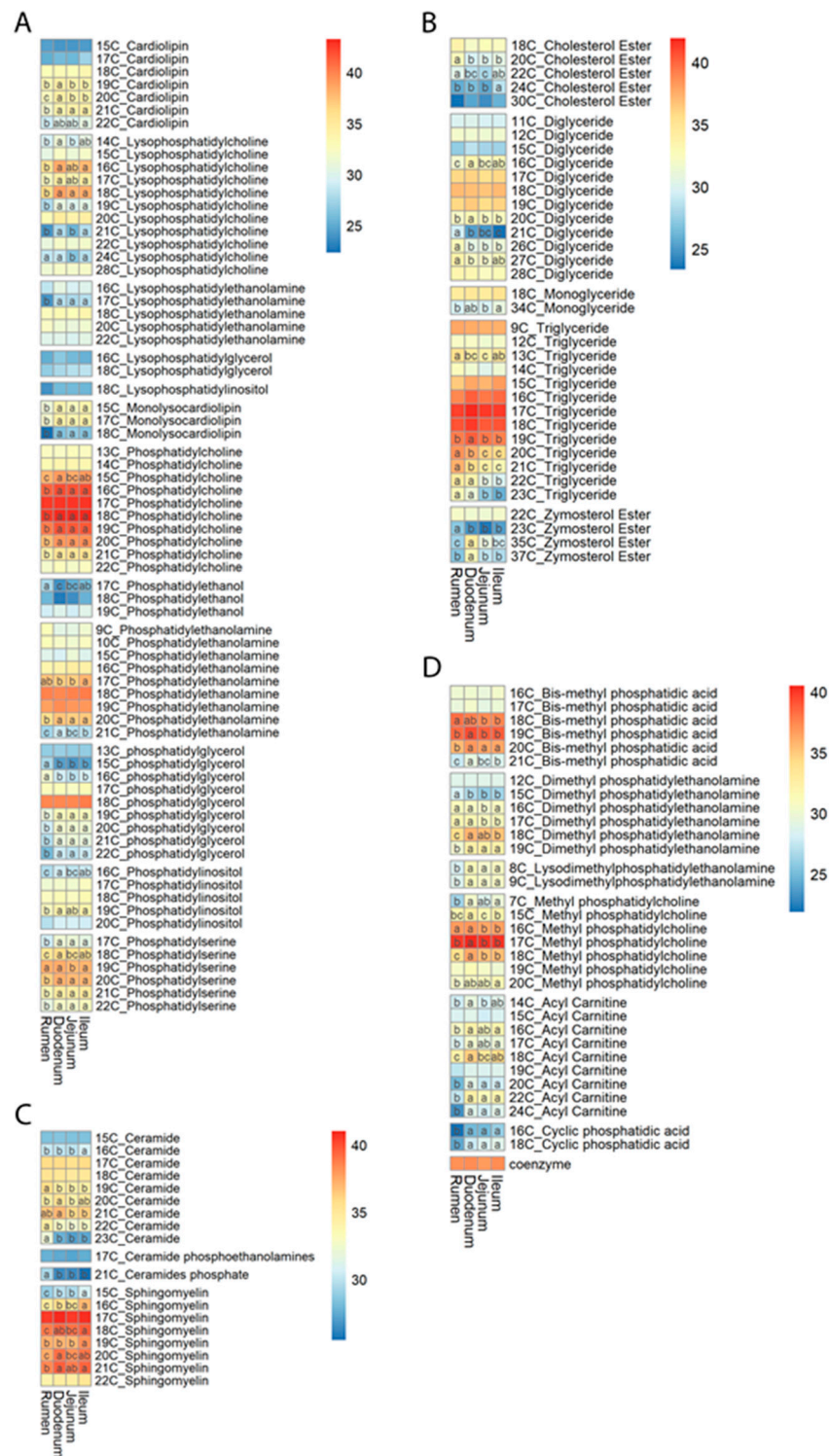


**Figure 3.** Signal counts of average fatty acid chain length in each lipid class across the ruminal papillae and epithelium from duodenum, jejunum, and ileum of 5 lactating Holstein cows ((A): phospholipids, (B) neutral lipids, (C) sphingolipids, (D) derivatized lipids, fatty acyl, and other lipids). The letter C and a number denote the average fatty acid chain length. Red denotes high signal counts, yellow median signal counts, and blue low signal counts in each lipid class. <sup>a,b,c</sup> Means with on the same row differ ( $p < 0.05$ ).

The major average degree of FA unsaturation ranged from 0 to 4 double bonds (Figure 4). However, species such as LPC, LPE, PC, PG, ChE, and MePC had up to five



18:0 [59]. Endogenous (De novo synthesis) lipids of microbial origin and the exogenous FA contribute to the total lipid content of bacterial dry mass in the rumen ranging from 10–15% [59]. The ruminal microbial lipids contain higher concentrations of SFA, especially C16:0 (18–23 g/100 g FA) and C18:0 FA (36–52 g/100 g FA), and USFA concentrations are low. The concentration of C18:1 and C18:2 range from 9–14 and 1.8–3.3 g/100 g FA. [61]. The lipidomic data showed the total FA chain length and degree of freedom in each lipid species. Each lipid species had one or more than one FA, and we do not know all the FA chain length and degree of freedom for each FA, making it difficult to compare with previous diet and microbiome FA composition. In the future, more lipidomic data from the diet and ruminal digesta could potentially help a comparison with the present data and help assess potential functional relevance for the GIT.

The shortage of the way of presenting chain length and unsaturation in Figures 3 and 4 is that FA chain length and degree of freedom were calculated by the sum dividing the number of FA and these numbers were rounded, and the possible chain length and unsaturation were recorded in the Supplementary File Table S7. However, we can still have a general idea about their chain length and unsaturation. Among these lipid species, most FA have 16–20 carbons, and ChE and ZyE were mainly attached to very long chain FA (more than 22 carbon). It is unknown, to our knowledge, if the FA absorbed from the lumen participates in the synthesis of ChE and ZyE in the GIT.

### 3.4. Lipid Ontology

Figure 5 depicts the lipid ontology in each term within LION. In the function category, the sum signal counts of lipid storage and lipid-mediated signaling were not significantly different (Figure 5A). The sum of signal counts of membrane components in the rumen was lower than the small intestine ( $p < 0.05$ ). The sum signal counts of ER, endosome, lysosome, and GA in the rumen were lower than in the intestine ( $p < 0.05$ ) (Figure 5B). The sum of signal counts in very low transition temperature, low transition temperature, average transition temperature, and high transition temperature in the small intestine were greater compared with the rumen (Figure 5C).

The lack of exact concentration of lipids based on the signal counts and the difference in the number of lipid species associated with each term precludes a direct comparison of LION terms in the same section of the GIT. However, we can compare differences for the same term across the various sections of the GIT. Based on the lipid species, LION helped us predict the functions, cell components, and cell characteristics. The DG can either be a signaling molecule or a membrane component in the LION classification, but the LION cannot separate specific functions. The greater sum of signal counts for membrane components and ER, endosome, lysosome, and GA in the intestine predicted that the intestine has a more complex membrane system, potentially due to its unique function in the absorption of nutrients. A more in-depth morphological analysis in the future could help ascertain this prediction.

Lipid phase transitions involve interconversions between various polymorphic (different solid structures formed by lipids) and mesomorphic (the intermediate phase between liquid and crystal) lipid phases. External variables such as temperature, water content, pressure, aqueous phase composition, and the chemical structure of lipids affect lipid self-assembly in different phases [63,64]. With the same FA, the PC transition temperature is lower than PE, and the shorter FA and the more UFA, the lower the transition temperature [63,64]. In the transition temperature category, the LION analysis included 299 lipid species among PC, PS, PG, PE, and SM. Details are provided in Supplementary File Table S8. Within the intestine, the duodenum had greater lipid signal counts associated with the very low transition temperature term.

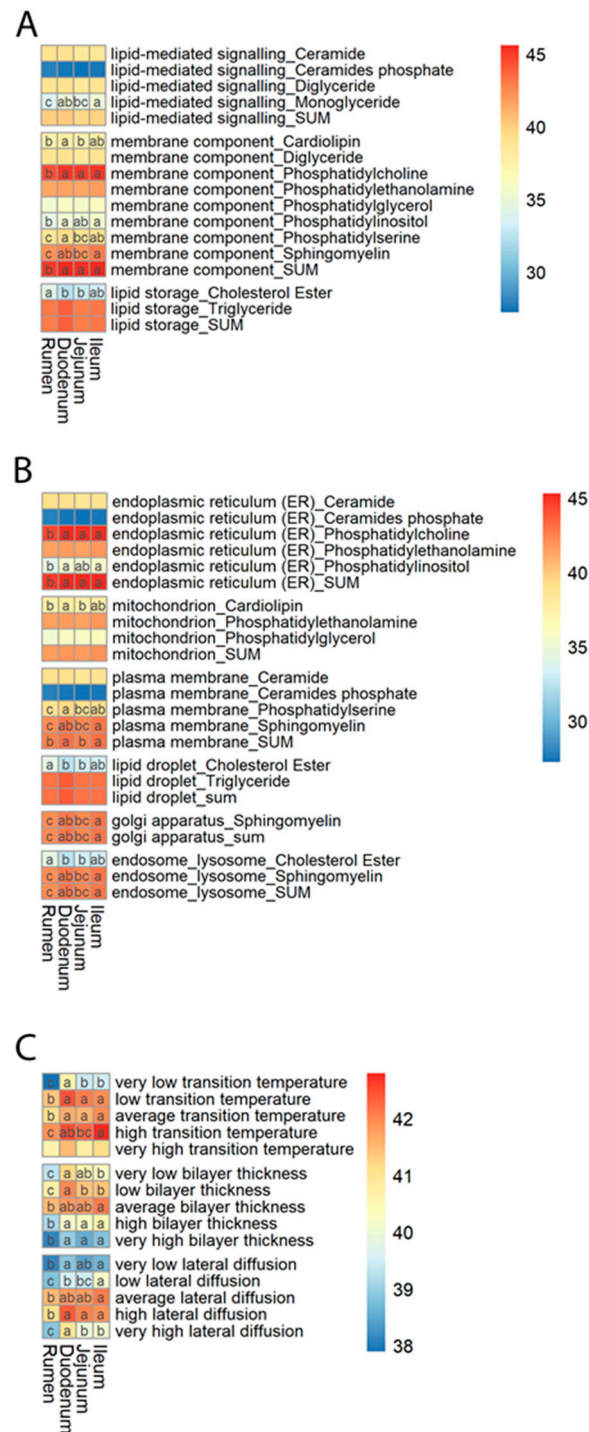


**Figure 5.** Signal counts of LION function terms in different LION term categories across the ruminal papillae and epithelium from duodenum, jejunum, and ileum of 5 lactating Holstein cows ((A) function, (B) cellular component, (C) transition temperature, bilayer thickness, and lateral diffusion.). Red denotes high signal counts, yellow median signal counts, and blue low signal counts in each lipid class. <sup>a,b,c</sup> Means with on the same row differ ( $p < 0.05$ ).

The sum of signal counts in the rumen for bilayer thickness were lower than in the intestine in each LION term associated with bilayer thickness. In the bilayer thickness category, the LION analysis included 213 lipid species among PC, PS, PG, and PE, and its classification is mainly based on the head group of lipids, FA chain length, and unsaturation. Within the intestine, the duodenum tended to have greater sum of signal counts of very

low and low bilayer thickness terms. There were no significant differences among average, high, and very high bilayer thickness, which predicted that the duodenum had a thinner bilayer thickness compared with the jejunum and ileum.

Lateral diffusion is a key parameter in evaluating membrane fluidity of the lipid bilayer membrane and the interaction between the bilayer lipid membrane and solid substrates [65]. In the lateral diffusion category, the LION analysis included 219 lipid species among PC, PS, PG, and PE. Similar to the bilayer thickness category, the sum of signal counts for each term in this category in the rumen was lower than in the intestine. In the very high lateral diffusion category, the duodenum had the highest sum of signal counts, followed by the jejunum and ileum, and the signal counts of the rumen were very low. This indicated that the small intestine had more lipid species related to lateral diffusion. The sum of signal counts of low lateral diffusion in the ileum were highest, and there was no significant difference in very low, average, and high lateral diffusion among the intestinal segments. The sum of signal counts of very high lateral diffusion in duodenum compared with jejunum and ileum predicted that the ileum had less lateral diffusion than the duodenum and jejunum. The same evaluation indicated that the duodenum had higher lateral diffusion than jejunum and ileum.

#### 4. Conclusions

For the first time, the lipid profiles across sections of the GIT have been determined using LC/MS/MS. We focused on these four sections because the rumen is the most important compartment in the forestomach, and the intestine is the major section where nutrient absorption occurs. Most of the lipid species that could be detected exist in all four sections of the lactating dairy cow GIT. The lipid composition of jejunum and ileum are very similar and differ markedly from the rumen and duodenum. Close to 50% of the lipid groups detected had a different profile across the four sections of the GIT. The average chain length of FA in the lipids detected ranged from 9 to 37 carbons, and the average degree of unsaturation ranged from 0 to 6. LION analysis predicted a more complex membrane system in the intestine than in the rumen, the duodenum had a thinner bilayer thickness among the small intestinal sections, and lateral diffusion ability was higher in the duodenum and lower in the ileum. A limitation of the present study was that the lipidomic data pertains to the whole tissue, disregarding the specific contribution of organelles. It was not feasible to ascertain if the differences in lipid profiles are partly associated with dietary or microbial sources. Due to the lack of published data, the functions and distribution of certain lipids in cells of the rumen could not be discerned. Future studies will have to be performed to better understand what factors (function or cellular component) in a given section of the GIT are related to the different lipid species.

**Supplementary Materials:** The following supporting information can be downloaded at <https://www.mdpi.com/article/10.3390/ruminants3010007/s1>: Table S1: ingredient composition of the diet; Table S2: LION terms and lipid identifiers; Table S3: lipid groups and classes; Table S4: Lipid species only existed only in rumen; Table S5: Lipid species that were in 2–3 sections of GIT; Table S6: variable importance point (VIP) score of PLS-DA; Table S7: average fatty acid chain and degree of unsaturation; Table S8: LION function.

**Author Contributions:** Conceptualization, Q.J. and J.J.L.; methodology, Q.J.; software, Q.J.; data curation, Q.J.; writing—original draft preparation, Q.J.; writing—review and editing, J.J.L.; visualization, Q.J.; supervision, J.J.L.; project administration, J.J.L.; funding acquisition, J.J.L. All authors have read and agreed to the published version of the manuscript.

**Funding:** This research received no external funding.

**Institutional Review Board Statement:** All experimental procedures were approved by the University of Illinois (Urbana-Champaign) Institutional Animal Care and Use Committee (no. 17166).

**Informed Consent Statement:** Not applicable.

**Data Availability Statement:** All data in this manuscript is available upon reasonable request to the corresponding author.

**Acknowledgments:** Qianming Jiang was the recipient of a fellowship from the China Scholarship Council (CSC) to perform her studies at the University of Illinois (Urbana). The authors thank Yusheng Liang for helping with the lipid extraction protocol. Appreciation is also extended to Can Yang, a candidate in Nuclear, Plasma and Radiological Engineering, at the University of Illinois Urbana-Champaign, for providing help with MATLAB analysis. The help of Danielle Sherlock and Ahmad Abdullah A. Aboragah during tissue collection are also appreciated.

**Conflicts of Interest:** The authors declare no conflict of interest.

## References

- Bloom, M.; Evans, E. Physical properties of the fluid lipid-bilayer component of cell membranes: A perspective. *Q. Rev. Biophys.* **1991**, *24*, 293–397. [[CrossRef](#)]
- English, A.R.; Zurek, N.; Voeltz, G.K. Peripheral ER structure and function. *Curr. Opin. Cell Biol.* **2009**, *21*, 596–602. [[CrossRef](#)] [[PubMed](#)]
- Pollard, T. *Cell Biology*, 4th ed.; Elyse O'Grady: Philadelphia, The Netherlands, 2023; pp. 237–250.
- Van Meer, G.; Voelker, D.R.; Feigenson, G.W. Membrane lipids: Where they are and how they behave. *Nat. Rev. Mol. Cell Biol.* **2008**, *9*, 112–124. [[CrossRef](#)] [[PubMed](#)]
- Kullenberg, D.; Taylor, L.A.; Schneider, M.; Massing, U. Health effects of dietary phospholipids. *Lipids Health Dis.* **2012**, *11*, 3. [[CrossRef](#)]
- Ghanem, M.; Lewis, G.F.; Xiao, C.T. Recent advances in cytoplasmic lipid droplet metabolism in intestinal enterocyte. *BBA-Mol. Cell Biol. Lipids* **2022**, *1867*, 159197. [[CrossRef](#)]
- Olzmann, J.A.; Carvalho, P. Dynamics and functions of lipid droplets. *Nat. Rev. Mol. Cell Biol.* **2019**, *20*, 137–155. [[CrossRef](#)]
- Nguyen, P.; Leray, V.; Diez, M.; Serisier, S.; Le Bloc'H, J.; Siliart, B.; Dumon, H. Liver lipid metabolism. *J. Anim. Physiol. Anim. Nutr.* **2008**, *92*, 272–283. [[CrossRef](#)] [[PubMed](#)]
- Raajendaran, A.; Tsiloulis, T.; Watt, M.J. Adipose tissue development and the molecular regulation of lipid metabolism. *Essays Biochem.* **2016**, *60*, 437–450.
- Merrill, A.H., Jr.; Sullards, M.C.; Wang, E.; Voss, K.A.; Riley, R.T. Sphingolipid metabolism: Roles in signal transduction and disruption by fumonisins. *Environ. Health Perspect.* **2001**, *109* (Suppl. 2), 283–289. [[PubMed](#)]
- Hla, T.; Dannenberg, A.J. Sphingolipid signaling in metabolic disorders. *Cell Metab.* **2012**, *16*, 420–434. [[CrossRef](#)]
- Braverman, N.E.; Moser, A.B. Functions of plasmalogen lipids in health and disease. *BBA-Mol. Basis Dis.* **2012**, *1822*, 1442–1452. [[CrossRef](#)]
- Kvidera, S.K.; Horst, E.A.; Sanz Fernandez, M.V.; Abuajamieh, M.; Ganesan, S.; Gorden, P.J.; Green, H.B.; Schoenberg, K.M.; Trout, W.E.; Keating, A.F.; et al. Characterizing effects of feed restriction and glucagon-like peptide 2 administration on biomarkers of inflammation and intestinal morphology. *J. Dairy Sci.* **2017**, *100*, 9402–9417. [[CrossRef](#)]
- Lin, Y.Y.; Gu, H.; Jiang, L.H.; Xu, W.; Liu, C.Q.; Li, Y.; Qian, X.Y.; Li, D.D.; Li, Z.L.; Hu, J.; et al. Cocaine modifies brain lipidome in mice. *Mol. Cell Neurosci.* **2017**, *85*, 29–44. [[CrossRef](#)] [[PubMed](#)]
- Zhang, H.Y.; Freitas, D.; Kim, H.S.; Fabijanic, K.; Li, Z.; Chen, H.Y.; Mark, M.T.; Molina, H.; Martin, A.B.; Bojmar, L.; et al. Identification of distinct nanoparticles and subsets of extracellular vesicles by asymmetric flow field-flow fractionation. *Nat. Cell Biol.* **2018**, *20*, 332–343. [[CrossRef](#)] [[PubMed](#)]
- Molenaar, M.R.; Jeucken, A.; Wassenaar, T.A.; van de Lest, C.H.A.; Brouwers, J.F.; Helms, J.B. LION/web: A web-based ontology enrichment tool for lipidomic data analysis. *Gigascience* **2019**, *8*, giz061. [[CrossRef](#)]
- Pang, Z.Q.; Zhou, G.Y.; Ewald, J.; Chang, L.; Hacariz, O.; Basu, N.; Xia, J.G. Using MetaboAnalyst 5.0 for LC-HRMS spectra processing, multi-omics integration and covariate adjustment of global metabolomics data. *Nat. Protoc.* **2022**, *17*, 1735–1761. [[CrossRef](#)]
- Klopp, R.N.; Ferreira, C.R.; Casey, T.M.; Boerman, J.P. Relationship of cow and calf circulating lipidomes with colostrum lipid composition and metabolic status of the cow. *J. Dairy Sci.* **2022**, *105*, 1768–1787. [[CrossRef](#)]
- Rico, J.E.; Saeed Samii, S.; Zang, Y.; Deme, P.; Haughey, N.J.; Grilli, E.; McFadden, J.W. Characterization of the Plasma Lipidome in Dairy Cattle Transitioning from Gestation to Lactation: Identifying Novel Biomarkers of Metabolic Impairment. *Metabolites* **2021**, *11*, 290. [[CrossRef](#)] [[PubMed](#)]
- Brasitus, T.A.; Dahiya, R.; Dudeja, P.K. Rat proximal small intestinal Golgi membranes: Lipid composition and fluidity. *Biochim. et Biophys. Acta (BBA)-Lipids Lipid Metab.* **1988**, *958*, 218–226. [[CrossRef](#)]
- Omodeo-Sale, F.; Lindi, C.; Marciani, P.; Cavatorta, P.; Sartor, G.; Masotti, L.; Esposito, G. Postnatal maturation of rat intestinal membrane: Lipid composition and fluidity. *Comp. Biochem. Physiol. Part A Physiol.* **1991**, *100*, 301–307. [[CrossRef](#)]
- Keelan, M.; Walker, K.; Thomson, A.B.R. Intestinal brush border membrane marker enzymes, lipid composition and villus morphology: Effect of fasting and diabetes mellitus in rats. *Comp. Biochem. Physiol. Part A Physiol.* **1985**, *82*, 83–89. [[CrossRef](#)] [[PubMed](#)]

23. Brasitus, T.A.; Dudeja, P.K.; Dahiya, R.; Halline, A. Dexamethasone-induced alterations in lipid composition and fluidity of rat proximal-small-intestinal brush-border membranes. *Biochem. J.* **1987**, *248*, 455–461. [[CrossRef](#)] [[PubMed](#)]
24. Schwarz, S.M.; Hostetler, B.; Ling, S.; Mone, M.; Watkins, J.B. Intestinal membrane lipid composition and fluidity during development in the rat. *Am. J. Physiol.* **1985**, *248*, G200–G207. [[CrossRef](#)] [[PubMed](#)]
25. Forstner, G.G.; Tanaka, K.; Isselbacher, K.J. Lipid composition of the isolated rat intestinal microvillus membrane. *Biochem. J.* **1968**, *109*, 51–59. [[CrossRef](#)]
26. Kaur, J. Chronic Ethanol Feeding Affects Intestinal Mucus Lipid Composition and Glycosylation in Rats. *Ann. Nutr. Metab.* **2002**, *46*, 38–44. [[CrossRef](#)] [[PubMed](#)]
27. Duranthon, V.; Frémont, L.; Léger, C.L. Effect of essential fatty acid deficiency on lipid composition of basolateral plasma membrane of pig intestinal mucosal cells. *Lipids* **1991**, *26*, 175–181. [[CrossRef](#)] [[PubMed](#)]
28. Daveloose, D.; Linaud, A.; Arfi, T.; Viret, J.; Christon, R. Simultaneous changes in lipid composition, fluidity and enzyme activity in piglet intestinal brush border membrane as affected by dietary polyunsaturated fatty acid deficiency. *Biochim. Biophys. Acta (BBA)-Lipids Lipid Metab.* **1993**, *1166*, 229–237. [[CrossRef](#)]
29. Lopez-Pedrosa, J.M.; Torres, M.I.; Fernández, M.I.; Ríos, A.; Gil, A. Severe Malnutrition Alters Lipid Composition and Fatty Acid Profile of Small Intestine in Newborn Piglets. *J. Nutr.* **1998**, *128*, 224–233. [[CrossRef](#)]
30. Schwarz, S.M.; Bostwick, H.E.; Danziger, M.D.; Newman, L.J.; Medow, M.S. Ontogeny of basolateral membrane lipid composition and fluidity in small intestine. *Am. J. Physiol.* **1989**, *257*, G138–G144. [[CrossRef](#)]
31. Hauser, H.; Howell, K.; Dawson, R.M.C.; Bowyer, D.E. Rabbit small intestinal brush border membrane. *Prep. Lipid Compos. Biochim. Biophys. Acta (BBA)-Biomembr.* **1980**, *602*, 567–577. [[CrossRef](#)]
32. Paradies, G.; Paradies, V.; Ruggiero, F.M.; Petrosillo, G. Role of Cardiolipin in Mitochondrial Function and Dynamics in Health and Disease: Molecular and Pharmacological Aspects. *Cells* **2019**, *8*, 728. [[CrossRef](#)]
33. Sparagna, G.C.; Lesnefsky, E.J. Cardiolipin remodeling in the heart. *J. Cardiovasc. Pharmacol.* **2009**, *53*, 290–301. [[CrossRef](#)]
34. Ren, M.; Phoon, C.K.; Schlame, M. Metabolism and function of mitochondrial cardiolipin. *Prog. Lipid Res.* **2014**, *55*, 1–16. [[CrossRef](#)]
35. Claypool, S.M. Cardiolipin, a critical determinant of mitochondrial carrier protein assembly and function. *Biochim. Biophys. Acta* **2009**, *1788*, 2059–2068. [[CrossRef](#)] [[PubMed](#)]
36. McBride, B.W.; Kelly, J.M. Energy cost of absorption and metabolism in the ruminant gastrointestinal tract and liver: A review. *J. Anim. Sci.* **1990**, *68*, 2997–3010. [[CrossRef](#)]
37. Cecilian, F.; Audano, M.; Addis, M.F.; Lecchi, C.; Ghaffari, M.H.; Albertini, M.; Tangorra, F.; Piccinini, R.; Caruso, D.; Mitro, N.; et al. The untargeted lipidomic profile of quarter milk from dairy cows with subclinical intramammary infection by non-aureus staphylococci. *J. Dairy Sci.* **2021**, *104*, 10268–10281. [[CrossRef](#)] [[PubMed](#)]
38. Zhao, Y.; Yu, S.; Zhao, H.; Li, L.; Li, Y.; Tu, Y.; Jiang, L.; Zhao, G. Lipidomic profiling using GC and LC-MS/MS revealed the improved milk quality and lipid composition in dairy cows supplemented with citrus peel extract. *Food Res. Int.* **2022**, *161*, 111767. [[CrossRef](#)] [[PubMed](#)]
39. Teng, Z.; Wang, L.; Du, H.; Yang, G.; Fu, T.; Lian, H.; Sun, Y.; Liu, S.; Zhang, L.; Gao, T. Metabolomic and Lipidomic Approaches to Evaluate the Effects of *Eucommia ulmoides* Leaves on Milk Quality and Biochemical Properties. *Front. Vet. Sci.* **2021**, *8*, 644967. [[CrossRef](#)]
40. Law, S.H.; Chan, M.L.; Marathe, G.K.; Parveen, F.; Chen, C.H.; Ke, L.Y. An Updated Review of Lysophosphatidylcholine Metabolism in Human Diseases. *Int. J. Mol. Sci.* **2019**, *20*, 1149. [[CrossRef](#)] [[PubMed](#)]
41. Pineiro, R.; Falasca, M. Lysophosphatidylinositol signalling: New wine from an old bottle. *Biochim. Biophys. Acta* **2012**, *1821*, 694–705. [[CrossRef](#)]
42. Makide, K.; Kitamura, H.; Sato, Y.; Okutani, M.; Aoki, J. Emerging lysophospholipid mediators, lysophosphatidylserine, lysophosphatidylthreonine, lysophosphatidylethanolamine and lysophosphatidylglycerol. *Prostaglandins Other Lipid Mediat.* **2009**, *89*, 135–139. [[CrossRef](#)] [[PubMed](#)]
43. Ikeda, I.; Imaizumi, K.; Sugano, M. Absorption and transport of base moieties of phosphatidylcholine and phosphatidylethanolamine in rats. *Biochim. Biophys. Acta* **1987**, *921*, 245–253. [[PubMed](#)]
44. Goodman, D.S. Cholesterol ester metabolism. *Physiol. Rev.* **1965**, *45*, 747–839. [[CrossRef](#)]
45. Chang, T.Y.; Li, B.L.; Chang, C.C.; Urano, Y. Acyl-coenzyme A:cholesterol acyltransferases. *Am. J. Physiol. Endocrinol. Metab.* **2009**, *297*, E1–E9. [[CrossRef](#)] [[PubMed](#)]
46. Steele, M.A.; Vandervoort, G.; AlZahal, O.; Hook, S.E.; Matthews, J.C.; McBride, B.W. Rumen epithelial adaptation to high-grain diets involves the coordinated regulation of genes involved in cholesterol homeostasis. *Physiol. Genom.* **2011**, *43*, 308–316. [[CrossRef](#)]
47. Aschenbach, J.R.; Penner, G.B.; Stumpff, F.; Gabel, G. Ruminant Nutrition Symposium: Role of fermentation acid absorption in the regulation of ruminal pH. *J. Anim. Sci.* **2011**, *89*, 1092–1107. [[CrossRef](#)]
48. Omoigui, S. Cholesterol synthesis is the trigger and isoprenoid dependent interleukin-6 mediated inflammation is the common causative factor and therapeutic target for atherosclerotic vascular disease and age-related disorders including osteoporosis and type 2 diabetes. *Med. Hypotheses* **2005**, *65*, 559–569.
49. Goodlad, R.A. Some effects of diet on the mitotic index and the cell cycle of the ruminal epithelium of sheep. *Exp. Physiol.* **1981**, *66*, 487–499. [[CrossRef](#)]

50. Japelt, R.B.; Jakobsen, J. Vitamin D in plants: A review of occurrence, analysis, and biosynthesis. *Front. Plant Sci.* **2013**, *4*, 136. [[CrossRef](#)]
51. Hoshino, Y.; Gaucher, E.A. Evolution of bacterial steroid biosynthesis and its impact on eukaryogenesis. *Proc. Natl. Acad. Sci. USA* **2021**, *118*, e2101276118. [[CrossRef](#)]
52. Li, Y.; Nicholson, R.J.; Summers, S.A. Ceramide signaling in the gut. *Mol. Cell Endocrinol.* **2022**, *544*, 111554. [[CrossRef](#)]
53. Uchida, Y. Ceramide signaling in mammalian epidermis. *Biochim. Biophys. Acta* **2014**, *1841*, 453–462. [[CrossRef](#)]
54. Morad, S.A.; Cabot, M.C. Ceramide-orchestrated signalling in cancer cells. *Nat. Rev. Cancer* **2013**, *13*, 51–65. [[CrossRef](#)]
55. Becker, K.A.; Tummeler, B.; Gulbins, E.; Grassme, H. Accumulation of ceramide in the trachea and intestine of cystic fibrosis mice causes inflammation and cell death. *Biochem. Biophys. Res. Commun.* **2010**, *403*, 368–374. [[CrossRef](#)]
56. Qu, Q.; Zeng, F.; Liu, X.; Wang, Q.J.; Deng, F. Fatty acid oxidation and carnitine palmitoyltransferase I: Emerging therapeutic targets in cancer. *Cell Death Dis.* **2016**, *7*, e2226. [[CrossRef](#)]
57. Yang, H.; Wang, X.; Xiong, X.; Yin, Y. Energy metabolism in intestinal epithelial cells during maturation along the crypt-villus axis. *Sci. Rep.* **2016**, *6*, 31917. [[CrossRef](#)] [[PubMed](#)]
58. Salvi, P.S.; Cowles, R.A. Butyrate and the Intestinal Epithelium: Modulation of Proliferation and Inflammation in Homeostasis and Disease. *Cells* **2021**, *10*, 1775. [[CrossRef](#)] [[PubMed](#)]
59. Jenkins, T.C. Lipid Metabolism in the Rumen. *J. Dairy Sci.* **1993**, *76*, 3851–3863. [[CrossRef](#)] [[PubMed](#)]
60. Vlaeminck, B.; Fievez, V.; Demeyer, D.; Dewhurst, R.J. Effect of forage:concentrate ratio on fatty acid composition of rumen bacteria isolated from ruminal and duodenal digesta. *J. Dairy Sci.* **2006**, *89*, 2668–2678. [[CrossRef](#)] [[PubMed](#)]
61. Bainbridge, M.L.; Cersosimo, L.M.; Wright, A.D.G.; Kraft, J. Rumen bacterial communities shift across a lactation in Holstein, Jersey and Holstein × Jersey dairy cows and correlate to rumen function, bacterial fatty acid composition and production parameters. *FEMS Microbiol. Ecol.* **2016**, *92*, 59. [[CrossRef](#)]
62. Contreras, G.A.; O’Boyle, N.J.; Herdt, T.H.; Sordillo, L.M. Lipomobilization in periparturient dairy cows influences the composition of plasma nonesterified fatty acids and leukocyte phospholipid fatty acids. *J. Dairy Sci.* **2010**, *93*, 2508–2516. [[CrossRef](#)] [[PubMed](#)]
63. Lee, A.G. Lipid phase transitions and phase diagrams I. Lipid phase transitions. *Biochim. Biophys. Acta (BBA)-Rev. Biomembr.* **1977**, *472*, 237–281. [[CrossRef](#)]
64. Roberts, G.C.K. European Biophysical Societies Association. In *Encyclopedia of Biophysics*, 1st ed.; Springer: Berlin, Germany, 2013; pp. 1841–1854.
65. Oshima, A.; Nakashima, H.; Sumitomo, K. Evaluation of Lateral Diffusion of Lipids in Continuous Membranes between Freestanding and Supported Areas by Fluorescence Recovery after Photobleaching. *Langmuir* **2019**, *35*, 11725–11734. [[CrossRef](#)] [[PubMed](#)]

**Disclaimer/Publisher’s Note:** The statements, opinions and data contained in all publications are solely those of the individual author(s) and contributor(s) and not of MDPI and/or the editor(s). MDPI and/or the editor(s) disclaim responsibility for any injury to people or property resulting from any ideas, methods, instructions or products referred to in the content.